AIAA AVIATION Forum
13-17 June 2016, Washington, D.C.
47th AIAA Plasmadynamics and Lasers Conference

Multiple aperture approach for the study of large-scale boundary-layer structures

Matthew R. Kemnetz* Robert Burns † and Stanislav Gordeyev ‡
University of Notre Dame, Notre Dame, Indiana, 46446, USA

An investigation of large-scale boundary layer structure using two simultaneously sampled streamwise oriented apertures is presented. Measurements were conducted in Notre Dame's Tri-Sonic facility at $M = 0.5$ at varying sampling frequencies and aperture separations. In this paper we investigate the convective nature of boundary layer structures using wavefront sensing techniques and POD analysis. The data has shown that the low order POD modes, corresponding to the larger structures within the flow, mostly convect and do so at a higher convective velocity. Despite the fact that higher order modes only account for $\approx 30\%$ of the energy in the wavefront, they contribute significantly in the residual wavefront error. For this reason, models beyond a linear, simply convecting model must be developed to accurately make wavefront predictions with separations greater than 3δ.

Nomenclature

δ	Boundary layer thickness
δ^*	Displacement thickness
θ	Momentum thickness
λ	Wavelength
ρ	Fluid density
OPD	Optical Path Difference
OPL	Optical Path Length
POD	proper Orthogonal Decomposition
$SHWFS$	Shack-Hartmann Wavefront Sensor
St_δ	Strouhal number based on δ
TWT	Tri-Sonic Wind Tunnel
U_c	Convective velocity

I. Introduction

Large-scale structures in turbulent boundary layers are of particular interest to researchers. Large-scale structures are important to boundary layer dynamics as they are responsible for entrainment processes and, via a link with small-scale structures near the wall, instantaneous drag near the wall.[1,2] While there exists a large body of experimental research concerning large-scale structures,[3–5] there remain open questions about their topology, dynamics, and their interaction with near-wall structures. Until recently, the experimental study of such topics has been difficult and limited.[6,7]

Large-scale structures are often difficult to investigate experimentally partially due to the trade-off between spatial resolution and region of interest. Fine spatial resolution enables the investigation of the fine

*Graduate Student, Department of Aerospace and Mechanical Engineering, Hessert Laboratory for Aerospace Research, Notre Dame, IN, 46556, AIAA Student Member.

†Graduate Student, Department of Aerospace and Mechanical Engineering, Hessert Laboratory for Aerospace Research, Notre Dame, IN, 46556, AIAA Student Member.

‡Research Associate Professor, Department of Aerospace and Mechanical Engineering, Hessert Laboratory for Aerospace Research, Notre Dame, IN, 46556, AIAA Associate Fellow.

details in the flow but inhibits the ability to capture the larger picture necessary to study large-scale structures. Usually, large scale structures are studied using various velocimetry techniques. Most notably they have been studied using hot wires (very fine spatial resolution and temporally resolved) and particle image velocimetry (PIV, time resolved velocity field) techniques. Alternatively, large scale structures can be studied non-intrusively by leveraging their inherent density distortions. When an otherwise collimated, coherent beam of light encounters a turbulent flow field that includes density fluctuations (compressible turbulent boundary layer; for example), its optical wavefront becomes aberrated. As planar wavefronts propagate through these unsteady density distributions, they become distorted and these distortions can be accurately measured by various wavefront sensors.[8,9] One very useful feature of these measurements is that they are non-intrusive by nature and be can be easily applied at high speeds,[10] including the hypersonic regime.[11] It is important to note that optical structures are closely related to physical turbulent structures but they are distinct. The optical quantity measured (OPD) is an integrated quantity; nonetheless, recent simultaneous PIV/Optical measurements[12,13] provided valuable insight into the investigation of large scale turbulent boundary layer structures.

As mentioned above, in order to fully characterize these large scale optical structures, a large aperture can be used. But, the use of a large aperture presents itself with its own challenges. Naturally, the use of a large aperture limits spatial resolution as the resolution of the wavefront sensor is fixed. In addition, as the aperture grows sensitivity to mechanical jitter also increases.[14] In this work, we look to investigate large-scale turbulent structures by measuring aero-optical distortions at two separate streamwise locations using a wavefront sensor. In this manner a larger aperture can be investigated by using smaller apertures.

This technique simultaneously measures the flow at different streamwise locations and provides important insight into the temporal-spatial evolution of large-scale structures. As wavefronts are the result of the integrated density field, which is in turn is governed by the Navier-Stokes equations, the spatial-temporal evolution of the wavefronts also follow deterministic physical laws and the proposed technique will help the development of future physics based models.

One place where this eventual physics-based model for wavefront evolution is critical is for adaptive optic control. Previous work by Burns et al.[15] has demonstrated that a major limiting factor for airborne adaptive optic systems is the cumulative latency inherent in the adaptive optic system. Time spent on digital calculations, physical sensor response, analog-to-digital conversion of sensor signals, electronic amplifiers, and electromechanical response of deformable mirrors all factor into the overall latency of the adaptive optic system.[15] This latency problem was approached by Burns et al. by developing a predictive controller. In this manner measurements were made over the aperture and the controller predicted forward in time. The control action is then performed based on the predicted flow characteristics. The latency tolerance is built into the prediction step.

Fundamentally, in the root of the latency problem lays the fact that for most AO systems the aero-optical distortions are commonly treated as unknown a priori, which requires an unrealistically-fast closed-loop adaptive-optics system. We propose that an alternative approach for a latency tolerant system would be to use multiple apertures and eventually, a physics-based model. A second aperture could be placed upstream of the lasing aperture and measurements would take place at this upstream location. By the time measurements finished, the flow structures would have convected over the main lasing aperture. Instead of measuring at one location and predicting forward in time, multiple apertures allow the use an upstream measurement as the prediction for the flow over the aperture. Currently this prediction is based upon Taylors frozen flow hypothesis. In this work we investigate the limits of Taylors frozen flow hypothesis and the assumption that boundary layer structures simply convect. In the future we would like to develop a more comprehensive model than simple structure convection, accounting for diffusion and production as well as non-linear interaction among the structures.

Finally, this work serves as a validation for previous work done in the study of large scale boundary layer structures. Previously, we developed several algorithms for recombining a wavefront in space from many measurements taken in time.[16] These techniques trade time for space based upon Taylors Frozen flow hypothesis. This work will demonstrate the limits of the previously developed algorithms.

II. Experimental Procedure

Wavefront data used in this work were collected in the Hessert Tri-sonic Wind Tunnel (TWT) at the University of Notre Dame. The TWT is a continuous flow indraft wind tunnel with an inlet contraction ratio

of 150:1. The test section used has a cross section of 10 cm 9.9 cm. The tunnel test section is constructed of Plexiglas. The test section was 160 cm in length from the end of the inlet to the diffuser. Optical access windows are installed on the upper and lower walls of the test section from 130 cm to 150 cm. Freestream velocity was measured using a static pressure port just upstream of the optical window and was held constant at M = 0.50 for the duration of the measurements. The boundary layer thickness, δ, at the measurements location was found to be approximately 15.6 mm, with δ^* to be about 2.4 mm and $\theta = 1.74$ mm. Based on these values we have $Re_\theta = 15,500$. Detailed description of the tunnel is provided in Smith.[17] A schematic of the experimental facility can be seen in Figure [1].

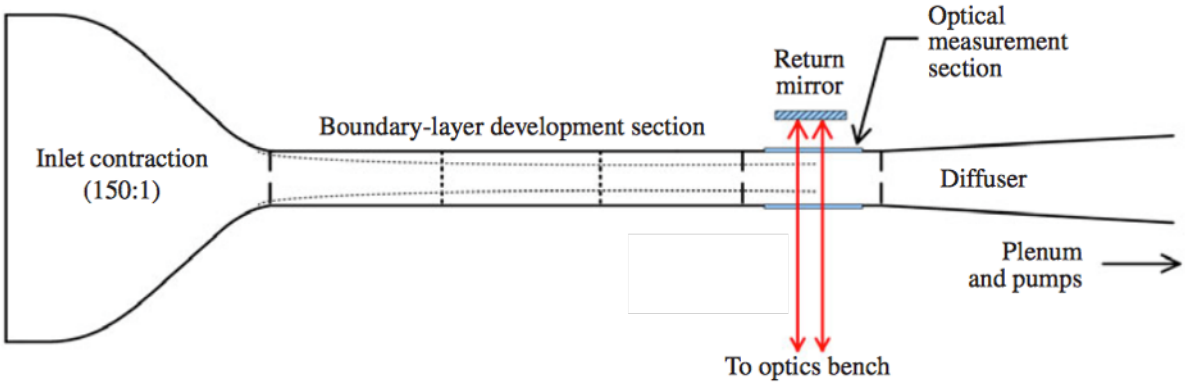

Figure 1. Schematic of the Notre Dame Tri-sonic Wind Tunnel Facility.

For this experiment the laser source was first sent through a 1 inch beam expander and then masked down to a square beam. The square beam was then expanded once again with a Mag = 5 telescope and split with a series of mirrors to create two spatially separated beams with aperture size 2 in x 2 in, as shown in Figure [2]. Each beam was sent through the test section normally to the wall. After being reflected off the return mirrors, both beams were sent back to the optical table along the same paths they came in, the so-called double-path set-up. Returning beams were split off using a cube beam splitter. Full 2-D wavefronts, resolved in both the streamwise (x) and the spanwise (z) directions, were collected using a high-speed Shack-Hartmann Wavefront Sensor (SHWFS).

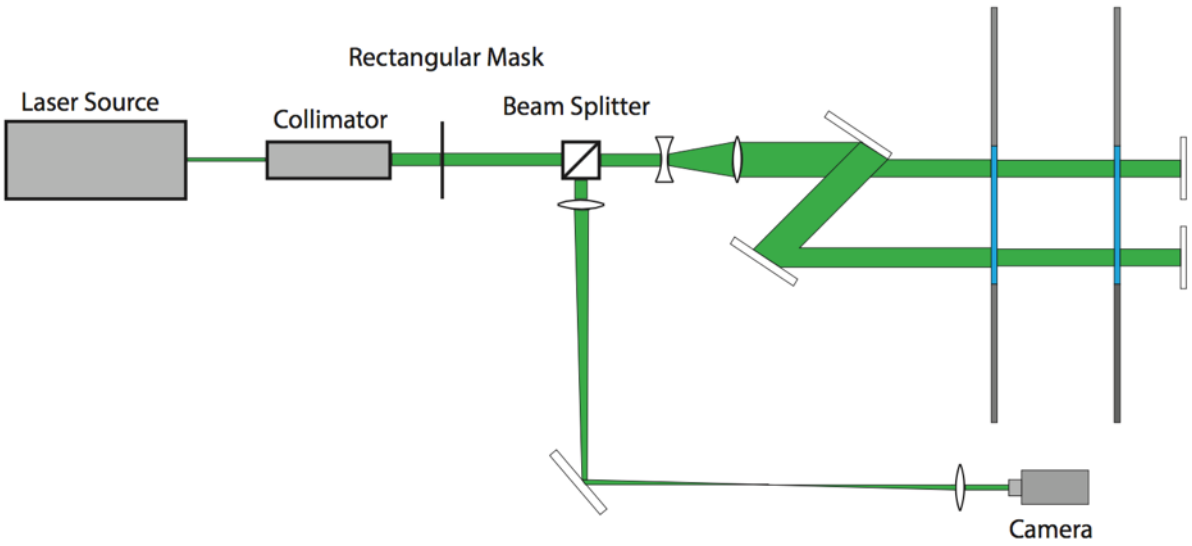

Figure 2. Schematic of the wavefront measurements using a 2-D Shack-Hartmann wavefront sensor.

Data was collected for beam separations of different streamwise distances between 3δ and 7δ.

Name	M	Subapertures	Separation	Sampling Frequency (Hz)
F1	0.5	22x22	3.30δ	77,064
F2	0.5	21x19	5.30δ	77,064
F3	0.5	15x22	7.25δ	77,064

Table 1. Experiment Matrix

Although the beams are traversed through two boundary layers on opposite sides of the test section, these boundary layers are statistically un-correlated and correct statistics for a single boundary layer can be extracted from these experiments.[9]

III. Results

III.A. Residual WF Error

To investigate the effect of beam separation we began by computing the residual WF error between the measured downstream wavefronts and the time-shifted upstream WFs. We define this quatity as the Global error, Σ.

$$\Sigma(\tau) = \frac{1}{T}\sum_{t}\frac{|WF_{UP}(t-\tau) - WF_{DN}(t)|^2}{OPD_{rms}^2} \tag{1}$$

In this manner upstream wavefronts were allowed to simply convect downstream and the error between the two wavefronts was computed. It is easy to show that varying the time-shift between wavefronts, τ, in Equation [1] is equivalent to varying the convective velocity of the upstream wavefront. The residual WF error plotted as a function of convective velocity can be seen in Figure [3].

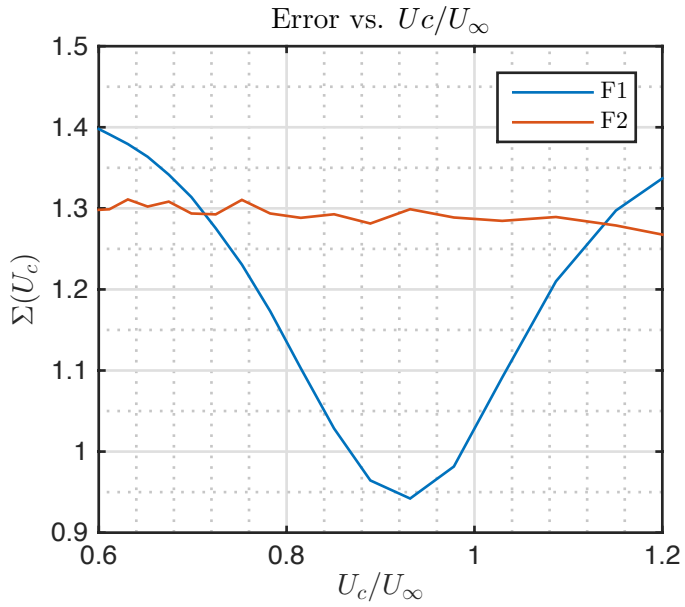

Figure 3. Plot of residual WF error vs. Convective velocity for F1 (separation = 3.30δ) and F2 (separation = 5.30δ) cases. $\Sigma_{min} = 0.928$ **at** $U_c/U_\infty = 0.932$

The error measured using Equation [1] was surprisingly high. Even for a modest separation of 3.3δ this immediately demonstrates that something beyond simple convection is at play. To better understand why the simply convecting model performed so poorly, we conducted POD analysis. In the remainder of this paper we will only be considering the F1 case.

III.B. POD Analysis

The wavefronts were decomposed into global modes using the POD technique[18]

$$W(x,z,t) = \sum_n a_n(t)\phi_n(x,z) \tag{2}$$

POD modes were computed for both the upstream and downstream apertures. No noticeable difference was found between the modes computed using the two different data sets. Modes computed from just the upstream aperture were used for the rest of the analysis.

We can begin by looking at how the different POD modes affect the frequency content of the overall wavefront.

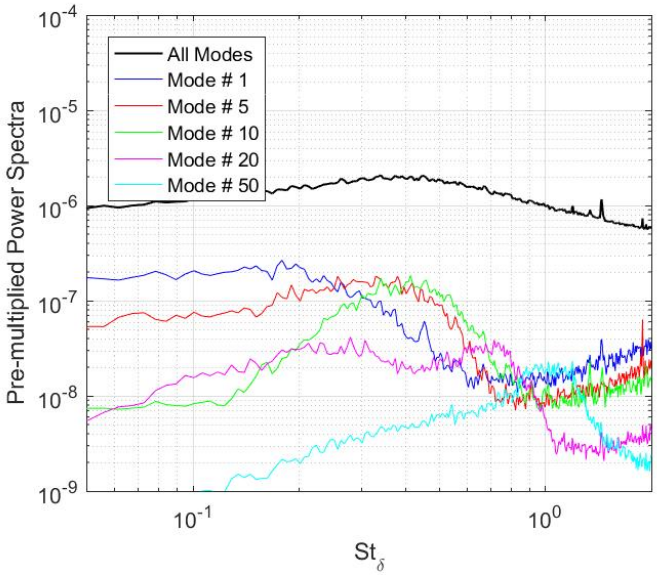

Figure 4. Pre-multiplied power spectra for the selected modes and for all POD modes.

Power spectra of the selected POD modes, pre-multiplied by the frequency, are shown in Figure [4], along with the overall pre-multiplied wavefront power spectrum. The energy contribution of the POD modes shifted toward higher frequencies, as the POD mode number increases; for instance, the peak contribution of the first mode is around $St_\delta = 0.2$, for mode 5 it is around $St_\delta = 0.4$ and mode 20 has its largest contribution around $St_\delta = 1$. There is significant energy buildup in the higher frequencies caused by spectral aliasing. Due to this energy buildup at higher frequencies the spectral method, or Malley Probe approach,[9] could not be used to compute convective velocity. Instead, wavefront error was computed using a direct cross-correlation of time-delayed wavefront POD coefficients. This was used to determine the convective velocity of individual POD modes.

The first 20 modes can be seen in Figure [5].

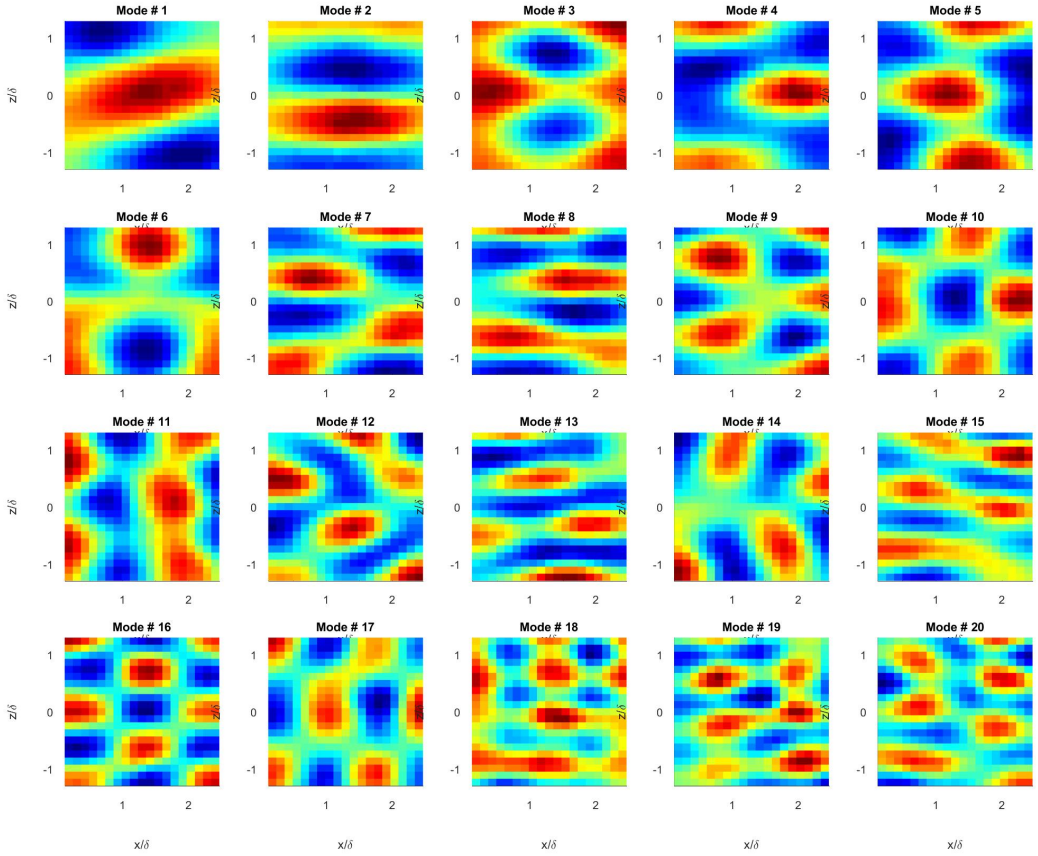

Figure 5. First 20 POD modes computed using the upstream aperture data.

A plot of the normalize eigenvalues and the cumulative eigenvalues can be seen in Figure [6].

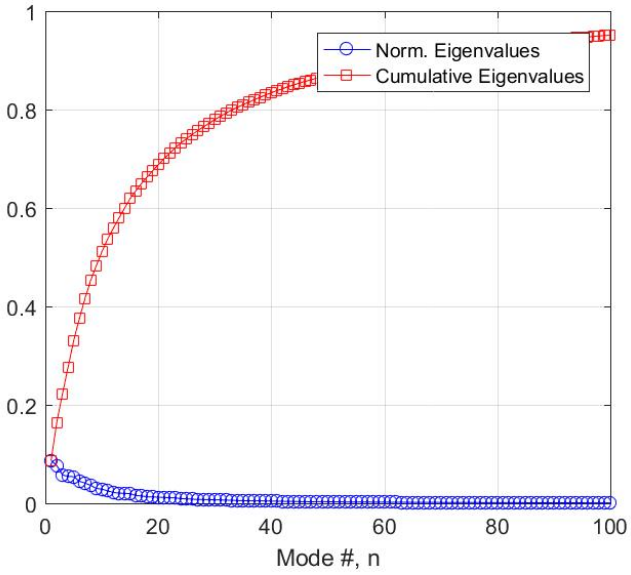

Figure 6. Normalized Eigenvalues vs. POD Mode number.

It is clear from Figure [6] that 80% of the energy of the wavefronts is contained in the first 30 modes. If we are to compare the error between upstream and downstream wavefronts as before, we have to introduce a new description of the error. We define the quantity relative error as

$$\epsilon(\tau, n) = \frac{1}{T} \sum_{t} \frac{|a_n^{UP}(t-\tau) - a_n^{DN}(t)|^2}{\lambda_n} \tag{3}$$

where $a_n(t)$ are the temporal coefficients defined in Equation [2] and λ_n is the total energy. The relative error, ϵ, and the global error due to the first n modes, $\Sigma(\tau, n)$ can be related,

$$\Sigma(\tau, n) = \frac{\sum_n [\epsilon(\tau, n)\lambda_n]}{\sum_n \lambda_n}. \tag{4}$$

It can easily be shown that in the limit of $n \to N$, where N is the total number of POD modes, Equation [4] is equivalent to Equation [1]. We can now compare the error using Equations [3] and [4] and compare the results. The relative error was computed with the first 20 POD modes. The first 20 POD modes correspond to the large scale, low frequency content in a wavefront.

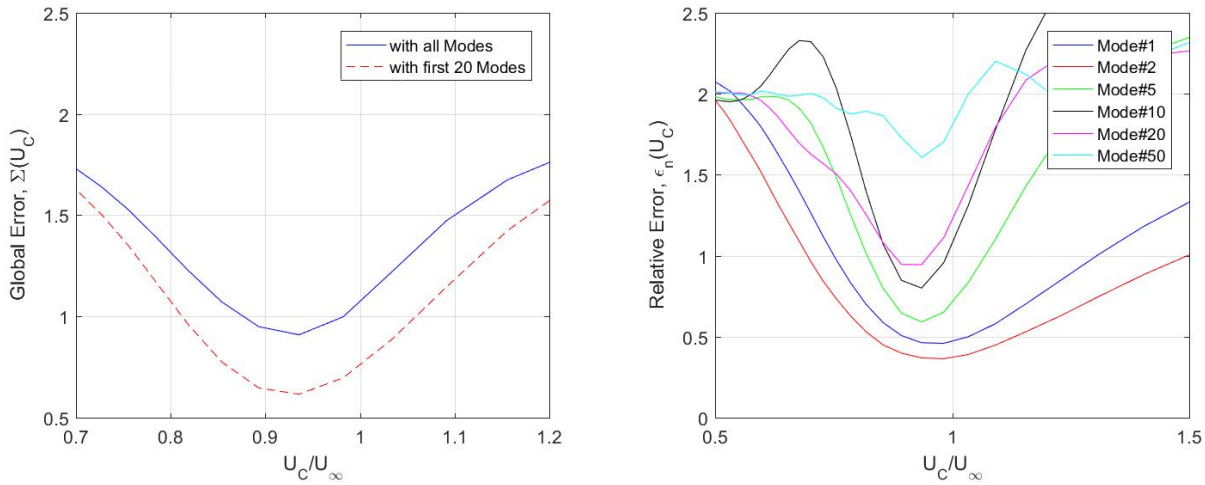

Figure 7. (a) Plot of residual WF error vs. Convective velocity for all POD modes and just the first 20 POD modes. (b) Residual Wavefront error for varying POD Modes.

There is a dramatic reduction in the residual wavefront error when just the first 20 POD modes are used. Despite the fact that the higher order modes (Mode # $>$ 20) account for just 30% of energy in the wavefront, they contribute significantly to the residual wavefront error. In Figure [7(b)] the relative error is plotted for various POD modes. One can clearly see the trend of significantly reduced relative error for the lower order POD modes. This implies that it is the lower order spatial modes that mostly convect while the higher order modes decay before reaching the downstream aperture. In the higher order modes there is simply no meaningful correlation between the upstream and downstream apertures.

In Figure [7(b)] one can also see the shift in the minimum error toward higher convective velocities for the lower order POD modes. In other words the low order modes pertaining to large scale structure within the boundary layer move with a higher convective velocity. This data is consistent with the idea that large scale structures primarily exist in the outer portion of the boundary layer and therefore convect at a higher speed.

A plot of the convective velocity for various mode numbers can be seen in Figure[8(a)]. The convective velocity for each mode number was computed by determining the minimum error between the time shifted upstream wavefront and the measured downstream wavefront.

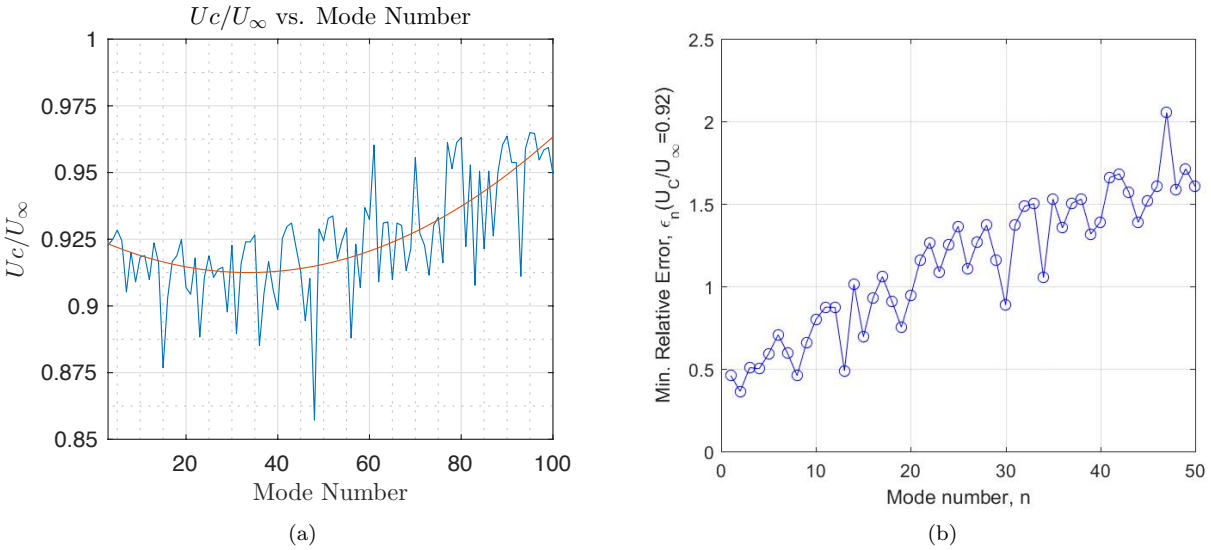

Figure 8. (a) Normalized convective velocity vs. Mode number. (b) Error vs. Mode Number.

A curve has been fit to the data in Figure[8(a)] just to demonstrate the general trend. As expected the low order modes move at a higher convective velocity. The higher order modes corresponding to smaller scale structures move with a slower convective velocity. For the highest modes the measured convective velocity increases again. We believe that trend is generally noise caused by a lack of correlation between the upstream and downstream data in these very high order modes. In addition, there is significant spread in the data which we believe could be caused by possible contamination from mechanical vibrations. As mentioned above, the direct method was used to compute the convective velocity of the individual POD modes. The direct method is more susceptible to contamination by mechanical vibration than the spectral method.

Now that we know how convective velocity varies for each mode, we can look at how the error varies with mode number. In Figure [8(b)] it can be seen how the low order POD modes convect downstream whereas the higher order modes do not. Higher order modes become completely uncorrelated by the time they reach the downstream aperture. It should also be noted that the very best performing modes, modes 2, 8, and 13 are comprised mostly of streamwise streaks in structure. This observation is consistent with the fact that large-scale structures that tend to convect over large distances[5–7] have predominantly streamwise-elongated topology

IV. Conclusion

Large scale boundary layer structures carry an important role in boundary-layer dynamics and as such they are of particular interest to researchers. In the past they have been primarily studied using hotwire and PIV techniques. In this work, measurements of aero-optical distortions due to turbulent boundary layers at two streamwise locations are presented and discussed. Measurements were conducted in Notre Dame's Tri-Sonic Wind Tunnel at $M = 0.5$ and various sampling frequencies and streamwise separations. The convective nature of the wavefront was investigated.

In this work we investigated the convective nature of the wavefront in order to verify previous work as well as test the limits of a simply convective assumption. We found that for a separation of $\approx 3\delta$ a simply convective model of wavefront propagation was not sufficient to characterize the downstream wavefront from upstream data. POD analysis showed that although the large scale structure of the wavefront primarily convects, the small scale structure of the wavefront is completely uncorrelated between the upstream and downstream apertures. These uncorrelated small scale structures are enough significantly reduce the predictive capabilities of a convective model for separations greater than 3δ.

One place where this work could be applied is in the area of adaptive optic control. Previous work by Burns et al.[15] has demonstrated that a major limiting factor for airborne adaptive optic systems is the cumulative latency inherent in the adaptive optic system. Time spent on digital calculations, physical sensor response, analog-to-digital conversion of sensor signals, electronic amplifiers, and electromechanical response of deformable mirrors all factor into the overall latency of the adaptive optic system.[15] Fundamentally, in the root of the latency problem lays the fact that for most AO systems the aero-optical distortions are commonly treated as unknown a priori, which requires an unrealistically-fast closed-loop adaptive-optics system. We propose that an alternative approach for a latency tolerant system would be to use multiple apertures and eventually, a physics-based model.

In order to improve upon the simply convective model, in the future we would like to investigate non-linear interactions between POD modes. As wavefronts were found to be related to the instantaneous velocity field9 it is reasonable to assume that since the POD representation of the velocity field can be represented as a sum of both linear and nonlinear terms10, the non-linear interaction between POD modes should also be included. Therefore, the effect of the non-linear interaction between the modes can be accounted as,

$$a_n^{DN}(t) \approx \sum_k \int_\tau A_{nk}(\tau) a_k^{UP}(t-\tau)\, d\tau + \sum_{k,m} \int_{\tau_1,\tau_2} B_{nkm}(\tau_1,\tau_2) a_k^{UP}(t-\tau_1) a_m^{UP}(t-\tau_2)\, d\tau_1\, d\tau_2 \qquad (5)$$

where the tensor $B_{nkm}(\tau_1, \tau_2)$ can also be found using a LSE technique. We believe that allowing for non-linear interaction between modes will improve our predictions for the larger separations.

References

[1]Hutchins, N. and Marusic, I., "Large-Scale Influences in Near-Wall Turbulence," *Philosophical Transactions: Mathematical, Physical and Engineering Sciences*, Vol. 365, No. 1852, 2007, pp. 647–664.

[2]Marusic, I., McKeon, B. J., Monkewitz, P. A., Nagib, H. M., Smits, A. J., and Sreenivasan, K. R., "Wall-bounded turbulent flows at high Reynolds numbers: Recent advances and key issues," *Physics of Fluids*, Vol. 22, No. 6, 2010.

[3]Smits, A. J., McKeon, B. J., and Marusic, I., "High-Reynolds Number Wall Turbulence," *Annual Review of Fluid Mechanics*, Vol. 43, 2011, pp. 353–375, http://dx.doi.org/10.1146/annurev-fluid-122109-160753.

[4]Bailey, S. C. C. and Smits, A. J., "Experimental investigation of the structure of large- and very-large-scale motions in turbulent pipe flow," *Journal of Fluid Mechanics*, Vol. 651, 5 2010, pp. 339–356.

[5]Hutchins, N. and Marusic, I., "Evidence of very long meandering features in the logarithmic region of turbulent boundary layers," *Journal of Fluid Mechanics*, Vol. 579, 2007, pp. 1–28.

[6]Dennis, D. J. C. and Nickels, T. B., "Experimental measurement of large-scale three-dimensional structures in a turbulent boundary layer. Part 1. Vortex packets," *Journal of Fluid Mechanics*, Vol. 673, 4 2011, pp. 180–217.

[7]Dennis, D. J. C. and Nickels, T. B., "Experimental measurement of large-scale three-dimensional structures in a turbulent boundary layer. Part 2. Long structures," *Journal of Fluid Mechanics*, Vol. 673, 4 2011, pp. 218–244.

[8]Gordeyev, S., Cress, J. A., Smith, A., and Jumper, E. J., "Aero-optical measurements in a subsonic, turbulent boundary layer with non-adiabatic walls," *Physics of Fluids*, Vol. 27, No. 4, 2015.

[9]Gordeyev, S., Smith, A. E., Cress, J. A., and Jumper, E. J., "Experimental studies of aero-optical properties of subsonic turbulent boundary layers," *Journal of Fluid Mechanics*, Vol. 740, 2014, pp. 214–253.

[10]Gordeyev, S., Hayden, T. E., and Jumper, E. J., "Aero-Optical and Flow Measurements Over a Flat-Windowed Turret," *AIAA Journal*, Vol. 45, No. 2, 02/01; 2016/01 2007, pp. 347–357, doi: 10.2514/1.24468; 05.

[11]Gordeyev, S. and Juliano, T. J., "Optical Characterization of Nozzle-Wall Mach-6 Boundary Layers," AIAA SciTech, American Institute of Aeronautics and Astronautics, 2016/01 2016, AIAA Paper 2016-1586.

[12]S. Gordeyev, A.E. Smith, T. S.-F. and McKeon, B., "Studies of the large-scale structure in adiabatic and moderately-wall-heated subsonic boundary layers," *Proceedings of the 9th International Symposium on Turbulence and Shear Flow Phenomena (TSFP-9)*, Paper 7A-3.

[13]Gordeyev, S. and Smith, A., "Studies of the Large-Scale Structure in Turbulent Boundary Layers Using Simultaneous Velocity-Wavefront Measurements," *46th AIAA Fluid Dynamics Conference*, AIAA-2016-3804.

[14]De Lucca, N. G., Gordeyev, S., Smith, A. E., Jumper, E. J., Whiteley, M., and Neale, T., "The Removal of Tunnel Vibration Induced Corruption in Aero-Optical Measurements," *45th AIAA Plasmadynamics and Lasers Conference*, AIAA Paper 2014-2494.

[15]Burns, W. R., Jumper, E. J., and Gordeyev, S., "A Latency-Tolerant Architecture for Airborne Adaptive Optic Systems," *53th AIAA Aerospace Sciences Meeting*, AIAA Paper 2015-0679.

[16]Kemnetz, M. R. and Gordeyev, S., "Optical investigation of large-scale boundary-layer structures," *54th AIAA Aerospace Sciences Meeting*, AIAA Paper 2016-1460.

[17]Smith, A. E., *Evaluation of passive boundary layer flow control techniques for aero-optic mitigation*, Ph.D. thesis, University of Notre Dame, 2015, Doctoral Dissertation.

[18]Holmes, Philip, H. P., *Turbulence, coherent structures, dynamical systems and symmetry*, Cambridge University Press, Cambridge, UK; New York, 2012, ID: 756045732.